https://ntrs.nasa.gov/search.jsp?R=19820014643 2020-03-21T08:27:49+00:00Z

General Disclaimer

One or more of the Following Statements may affect this Document

- This document has been reproduced from the best copy furnished by the organizational source. It is being released in the interest of making available as much information as possible.

- This document may contain data, which exceeds the sheet parameters. It was furnished in this condition by the organizational source and is the best copy available.

- This document may contain tone-on-tone or color graphs, charts and/or pictures, which have been reproduced in black and white.

- This document is paginated as submitted by the original source.

- Portions of this document are not fully legible due to the historical nature of some of the material. However, it is the best reproduction available from the original submission.

Produced by the NASA Center for Aerospace Information (CASI)

Center for Aeronautical Research

Bureau of Engineering Research
The University of Texas at Austin
Austin, Texas

(NASA-CR-162001) MODAL VECTOR ESTIMATION FOR CLOSELY SPACED FREQUENCY MODES (Texas Univ. at Arlington.) 41 p HC A03/MF A01 CSCL 20K
N82-22517
Unclas
G3/39 09618

Report CAR 82-1

MODAL VECTOR ESTIMATION FOR

CLOSELY-SPACED-FREQUENCY MODES

by

Roy R. Craig, Jr.
Yung-Tseng Chung
Mark Blair

NASA Contract No. NAS8-33980
February 1, 1982

APR 1982
RECEIVED
NASA STI FACILITY
ACCESS DEPT.

MODAL VECTOR ESTIMATION FOR CLOSELY-SPACED-FREQUENCY MODES

A Report to

NASA Marshall Space Flight Center

Contract No. NAS8-33980

by

Roy R. Craig, Jr.*

Yung-Tseng Chung†

Mark Blair††

ASE-EM Department

The University of Texas at Austin

Austin, Texas 78712

* Professor, ASE-EM

† Graduate Student, EM

†† Undergraduate Student, ASE

February 1, 1982

MODAL VECTOR ESTIMATION FOR CLOSELY-SPACED-FREQUENCY MODES

1. Introduction

In describing the dynamical behavior of a complex structure modal parameters are often employed: undamped natural frequency, mode shape, modal mass, modal stiffness, and modal damping. From both an analytical standpoint and an experimental standpoint, identification of modal parameters is made more difficult if the system has repeated frequencies or even closely-spaced frequencies. The more complex the structure, the more likely it is to have closely-spaced frequencies. In many cases this fact makes it difficult to determine valid mode shapes using single-shaker test methods. By employing band selectable analysis (zoom) techniques and by employing Kennedy-Pancu circle fitting or some multiple degree of freedom (MDOF) curve-fit procedure, the usefulness of the single-shaker approach can be extended. However, for many structures such procedures may still not be sufficient to give accurate modal representations.

It is the purpose of this paper to discuss techniques for obtaining improved modal vector estimates for systems with closely-spaced-frequency modes.

2. Closely-Spaced-Frequency-Modes

It is well-known that systems with unique frequencies possess unique mode shapes, while systems with repeated frequencies do not possess unique modes corresponding to the repeated frequencies, but rather, they possess

subspaces of modes. This is illustrated by the simple 2 degree-of-freedom (DOF) systems of Figure 1. Figure 2(a) shows the frequency response functions (FRF's) of a 2DOF system with widely-separated-frequency modes (5.0Hz and 5.5Hz), while Figure 2(b) shows a similar system with closely-spaced-frequency modes (5.00Hz and 5.05Hz).

The frequency spacing of the 2DOF system in Figure 2 is controlled by the strength of the coupling spring. Klosterman[1] made a thorough investigation of the dynamics of weakly coupled systems, such as the types illustrated in Figure 3, and concluded that, for such systems, "close agreement between computed and experimentally measured mode shapes cannot be expected." This results from the fact that "coupled system mode shapes are very sensitive to small variations in the subsystems." Table 1 illustrates the effect of small variations in the mass of one subsystem on the coupled system modes of a 2DOF spring-mass oscillator when the coupling is "weak." It can be seen that, as noted by Klosterman, small changes in the subsystem properties have an enormous effect on the system modes when the system consists of weakly coupled subsystems.

Figures 4 and 5 show FRF's of a moderately complex piece of space hardware. Figure 4 shows the Bode plot of a drive-point FRF over the full data acquisition bandwidth, while Figures 5(a) and 5(b) show two Argand plots over a 10-30Hz bandwidth. Clearly, this structure has closely-spaced-frequency modes. In actual fact, the structure is comprised of a tubular framework supporting several virtually identical honeycomb panels. Thus, this structure is a classic example of a system which consists of weakly-coupled subsystems.

Although Klostermann has noted that getting experimentally determined modes to agree with analytically determined modes may be a hopeless undertaking, we will address the slightly different proposition of determining "good" (in some sense) experimental modes for systems having closely-spaced frequencies.

3. Modal Vector Estimation Using a Single Column/Row of the Frequency Response Function Matrix

Techniques for estimating experimental mode shapes by using a single column or a single row of the FRF matrix are well known and are incorporated in various modal analysis software packages such as MODAL-PLUS. Appendix A gives the mathematical basis for using a single row/column of the FRF matrix in identifying modal parameters. The most frequently employed techniques for estimating modal vectors from FRF's are the quadrature response method and the Kennedy-Pancu circle-fit method.[2,3] Figure 6(a) shows the correct modes of the 2DOF systems of Figures 2(a) and 2(b) along with the quadrature response "experimental" modes which would be inferred from frequency response functions. When the frequencies are not closely spaced, acceptable results are obtained by the quadrature response technique, as seen in Figure 6(b). However, when the frequencies are closely spaced, there is difficulty, first, in identifying the natural frequencies at which to identify the modes; and modes based on one shaker location do not agree with modes based on another shaker location, as can be seen by comparing Figures 6(c) and 6(d).

The use of quadrature response techniques in situations where frequencies are closely spaced clearly leads to erroneous modal vector estimates. It could be shown that even circle-fitting and MDOF curve fitting would fail to produce good modal vector estimates in cases such as this.

Because of the difficulties in obtaining accurate modal vectors for systems with closely-spaced-frequency modes by using only a single column or row of the FRF matrix, it becomes necessary to examine the possibility of using several rows/columns of the FRF matrix to obtain improved modal vector estimates.

4. Modal Vector Estimation Using Several Columns/Rows of the Frequency Response Function Matrix

Figure 6 illustrates the difficulty in obtaining valid mode shapes from single-shaker data when the system has closely-spaced-frequency modes. If only one shaker location is employed, some modes may not be excited at all, and there may be superposition of contributions of several closely-spaced-frequency modes leading to inaccurate modal estimates. If additional shaker locations are employed, there may be ambiguity as to which shaker location gives the best estimate of a certain mode. Several techniques have been employed to combine the information from several rows/columns of the FRF matrix. These include:

- Modal Vector Weighting
  - Symmetry/Antisymmetry Weighting
  - Analytical Mode Weighting[4]

Ad Hoc Sort Logic Averaging[5]

Modal Tuning; Force Appropriation

- Asher Method[6-9]
- Extended Asher Method[10]
- Minimum Coincident Response Method[11]

Multishaker Sine Dwell Testing[12]

Figures 7(a) and 7(b) illustrate the problems caused by the superposition of the effects of closely-spaced-frequency modes. In Figure 7(a) it is seen that the presence of two modes is masked, and it appears that a single mode with greater amplitude and greater damping, or possibly even nonlinear effects, is present. Figure 7(b) shows the effect of mode superposition on a non-driving-point FRF. Here two modes are clearly evident, but the apparent amplitude of each mode is reduced from its true value. The methods listed above may be employed in an attempt to separate out the contributions of individual modes in such situations.

Figure 8 illustrates the basis of symmetry/antisymmetry averaging. Ground vibration testing of aircraft frequently employs symmetric/antisymmetric shaker configurations because of the inherent symmetry of the structure. Even so, there may be many closely-spaced-frequency modes in either the symmetric or the antisymmetric set of modes of an aircraft.

From Equations (A-7) and (A-10) it can be seen that, when the system has distinct roots, p_k, every row and column of the residue matrix a_k contains the modal vector u_k multiplied by a component of itself.

Richardson and Kniskern[5] extended the sort logic employed in producing mode shapes from a single row or column of the residue matrix and proposed a sort logic which would make use of data from multiple rows/columns of the residue matrix. Although they demonstrated some improvement in modal vector estimation, they recognized that their sort algorithm was based on "rather arbitrary rules," and that other "more 'optimum'" approaches might be possible.

Modal tuning, or force appropriation, is a third approach to employing multiple columns or rows of the FRF matrix to obtain system modes. The name "Asher method" is frequently applied to one such version of modal tuning. Extensive research has been done on this method in France, where the technique is referred to as "force appropriation." Reference 9 is just one of a number of the French papers dealing with the use of force appropriation for modal vector estimation.

The Asher method of modal tuning is based on the fact that when a system is excited at an undamped natural frequency ω_r by the appropriate force vector F_r, the response will be in quadrature with the excitation, and the quadrature response will correspond to the undamped natural mode ϕ_r.[6] That is, for monophase harmonic excitation of an nDOF system,

$$\underset{n\times 1}{X} = \underset{n\times n}{H}\ \underset{n\times 1}{F} = (H_R + iH_I)F \qquad (1)$$

For the response to be in quadrature with the excitation

$$H_R F = 0 \quad . \qquad (2)$$

Thus, the natural frequencies are determined from the condition that

$$\det(H_R(\omega_r)) = 0 \quad , \qquad r = 1, 2, \ldots , n \tag{3}$$

The force vector F_r required to tune the mode is given by Equation (2). Finally, the mode corresponding to the frequency ω_r is given by

$$X(\omega_r) = iH_I(\omega_r)F_r \tag{4a}$$

or

$$\phi_r = H_I(\omega_r)F_r \tag{4b}$$

Figure 9 shows the mechanics of how Asher tuning employs two columns of a FRF matrix to tune a mode.

In Equations (1) through (4) and in the example presented in Figure 9, it was assumed that all columns of the FRF matrix were available, i.e. that there could be forces imposed at all points where displacement (velocity, acceleration) measurements were made. In actual fact, the number of possible excitation points, p , is usually one or two orders of magnitude smaller than the number of response points, n .† In this case, Equations (1) through (4) are modified as follows:

$$\underset{p\times 1}{\hat{X}} = \underset{p\times p}{\hat{H}} \; \underset{p\times 1}{\hat{F}} \qquad p < n \tag{5}$$

$$\hat{H}_R \hat{F} = 0 \tag{6}$$

†Here it will be assumed that n , the number of response points, is sufficiently large to constitute the "order of the system" as far as the behavior of the system in the frequency range of interest is concerned.

$$\det(\hat{H}_R(\omega)) = 0 \rightarrow \hat{\omega}_r \tag{7}$$

$$\hat{X}(\hat{\omega}_r) = i\hat{H}_I(\hat{\omega}_r)\hat{F}_r \rightarrow \hat{\phi}_r \tag{8}$$

In Reference 7 it is shown that the frequencies and mode shapes obtained by applying Equations (5) through (8) to a $p \times p$ subset of the FRF matrix are frequently good approximations to the true frequencies and modes, but that "spurious modes" may also be produced when $p<n$. Modal tuning according to Equations (5) through (8) will be referred to as "standard Asher" (SA) tuning. Examples of standard Asher tuning will be presented in Section 5.

As noted, when the number of excitation points is small, i.e. $p \ll n$, the use of standard Asher tuning may lead to "spurious modes." These will have a response in quadrature with the excitation at the p excitation points, but at other measurement points the response may have a significant coincident component, thus giving the appearance of a "complex mode." Several approaches have been suggested for employing a non-square submatrix of the FRF matrix.[10,11] The technique proposed by Ensminger and Turner[11] may be referred to as the "minimum coincident response (MCR) method." Thus, for harmonic excitation,

$$\underset{m\times 1}{\tilde{X}} = \underset{m\times p}{\tilde{H}} \; \underset{p\times 1}{\tilde{F}} = (\tilde{H}_R + i\tilde{H}_I)\tilde{F} \qquad \begin{matrix} p \ll n \\ m \leq n \end{matrix} \tag{9}$$

$$\tilde{X}_R = \tilde{H}_R\tilde{F} \tag{10}$$

Let the coincident response norm be defined by

$$\varepsilon = \tilde{X}_R^T \tilde{X}_R \tag{11}$$

Then, the force vector $\tilde{F}$ is appropriated such that ε is minimized subject to an amplitude constraint. That is, $\tilde{F}(\omega)$ and $\varepsilon(\omega)$ are determined as functions of ω only by determining an expression for the $\hat{F}(\omega)$ which minimizes ε subject to an amplitude constraint.

$$\left.\begin{array}{l} \text{Min } \varepsilon\ (\tilde{F}(\omega)) \\ X_{iI} = 1 \end{array}\right\} \rightarrow \tilde{F}(\omega)\ ,\ \varepsilon(\omega) \tag{12}$$

where X_{iI} is the quadrature response at the ith response point. This results in a force vector given by

$$\tilde{F} = \frac{1}{\tilde{H}_{iI}(\tilde{H}_R^T\tilde{H}_R)^{-1}\tilde{H}_{iI}^T}\ (\tilde{H}_R^T\tilde{H}_R)^{-1}\ \tilde{H}_{iI}^T \tag{13}$$

where $\tilde{H}_{iI}$ is the ith row of the imaginary part of the FRF matrix. Finally, the frequencies $\tilde{\omega}_r$ are selected to minimize $\varepsilon(\omega)$, Equation (13) is used to compute the corresponding $\tilde{F}_r$, and the mode shape is determined from the quadrature response

$$\tilde{X}_I = i\tilde{H}_I(\tilde{\omega}_r)\tilde{F}_r \tag{14}$$

Ensminger and Turner reported good results from the application of the minimum coincident response method to synthesized frequency response functions based on ground vibration test data obtained for the mated 747-Space Shuttle Orbiter. They also applied the standard Asher method, Equations (5) through (8), to the same synthesized FRF's. They concluded that "this approach (i.e. the minimum coincident response method) was found to provide more consistent results than that based on direct determination of roots of the real part of the transfer function matrix (i.e. the standard Asher method)." Gold and Hallauer[8] discussed the application of the standard Asher method to synthesized FRF's, but were unable to successfully apply the method to actual experimental data.

5. Modal Tuning Applications

A research program is being conducted to evaluate the use of the standard Asher method and the minimum coincident response method in estimating modal vectors of systems having closely-spaced-frequency modes.[13] The specific questions being addressed are:

(1) Is modal tuning using either the standard Asher(SA) method or the minimum coincident response(MCR) method effective in producing modal vector estimates in situations where the results of single shaker methods are not adequate?

(2) How do the modal vector results obtained by the (SA) method and the (MCR) method compare?

(3) What is the effect of the frequency resolution used in the synthesis of FRF's on the modes produced by the SA method and the MCR method?

(4) How can residuals be employed in the synthesized FRF's used as input to the modal tuning methods?

Although work is still in progress on this research project, some tentative results in response to questions (1) through (3) will be presented. Figure 10 shows a flow chart of the major steps employed in the modal tuning studies.

Figure 11 shows a coupled-beam model which permitted experimental data to be acquired for a system with closely-spaced-frequency modes. Figure 12 shows a typical FRF and the results of using the MDOF curve-fit procedure in MODAL-PLUS (the GE and GA commands). The original experimental bandwidth was 10 Hz, which concentrated the spectrum around the lowest pair of closely-spaced-frequency modes. Table 2 gives the MDOF curve-fit results for the eight FRF's (2 reference points, 4 response points). From Table 2 the following may be noted:

(a) Each FRF has two dominant roots in the 118-121 Hz range.

(b) Some of these dominant roots have phase angles significantly different than $\pm 90^{\circ}$.

(c) The "modes" based on having a single shaker at 1 appear to be at approximately 119.0 Hz and 119.5 Hz; while the "modes" based on having a single shaker at 6 appear to be at 118.8 Hz and 120.0 Hz. However, the 119.0 Hz "mode" is radically different than the 118.8 Hz "mode."

The MDOF results presented in Table 2 were used as input to a program which first synthesizes analytical FRF's and then employs the

synthesized FRF's as input to the SA and MCR modal tuning algorithms. The modal tuning results for bandwidths of 10 Hz and 0.256 Hz are shown in Figures 13 and 14 respectively, and the results for several bandwidths are given in Table 3. From Table 3 the following may be noted:

(a) Two modes at approximately 118.8 Hz and 119.0 Hz are consistently identified by both methods.

(b) Reducing the analysis bandwidth reduces the phase error of the identified modes.

(c) The mode at 118.8 Hz appears to be much better than the mode at 119.0 Hz, i.e. there appears to be less phase error. However, it should be noted that the large phase errors in mode 2 are associated with relatively small amplitudes. In Figures 13(b) and 14(b) it may be noted that the minimum of $\varepsilon(\omega)$ is much less sharp for the 119.0 Hz mode than for the 118.8 Hz mode. This sharpness may be related to the phase coherence of the mode, but this relationship has not been thoroughly evaluated.

(d) For the 118.8 Hz mode there is good agreement between the SA mode and the MCR mode. For the second mode the agreement is not so good.

(e) The tuned modes do not exhibit the symmetrical antisymmetric behavior which was expected because of the apparent symmetry of the structure. The explanation for this discrepancy may lie in the mode sensitivity of weakly coupled systems as previously discussed.

Attempts to employ the SA modal tuning technique on some of the data from the structure whose FRF's are shown in Figures 4 and 5 indicated that

it would be necessary to include residuals in the synthesized FRF's. Work on residuals is in progress and no results are yet available.

6. Conclusions

On the basis of the research described above, the following conclusions may be stated:

(a) Standard Asher tuning and minimum coincident response tuning both provide rational means for employing multiple rows or columns of the FRF matrix to improve modal vector estimates.

(b) The use of synthesized frequency response functions rather than original experimental FRF's has two advantages: (1) far less memory is required to store the synthesis parameters than is required to store a complete FRF, and (2) the analysis bandwidth can be reduced to obtain better estimates of the modal vectors.

(c) Much additional research is needed, particularly in three areas: (1) application of modal tuning to testing of more complex structures, (2) use of synthesized FRF's for reference points where no actual shakers were located, and (3) use of residuals where modal density is very large.

7. Appendix A - Single Column/Row Methods of Modal Parameter Identification

References 2 through 4, and many other papers, describe the basis for using a single column or row of the FRF matrix to estimate modal parameters. It is assumed that the motion of the physical system can be adequately described by a set of simultaneous second-order linear differential equations of the form

$$M\ddot{x}(t) + C\dot{x}(t) + Kx(t) = f(t) \qquad \text{(A-1)}$$

where

$x(t)$ = system displacement vector (nx1)

$f(t)$ = force vector

M = mass matrix

C = damping matrix

K = stiffness matrix

It is convenient to take the Laplace transform of Equation (A-1) giving

$$B(s)\,X(s) = F(s) \qquad \text{(A-2)}$$

where

$X(s)$ = Laplace transform of displacement vector

$F(s)$ = Laplace transform of force vector

$B(s)$ = $Ms^2 + Cs + K$

s = (complex) Laplace variable

Equation (A-2) can also be written in the form

$$X(s) = H(s)F(s) \qquad \text{(A-3)}$$

where

$$H(s) = (B(s))^{-1} \qquad \text{(A-4)}$$

$H(s)$ is referred to as the transfer matrix. $H(s=i\omega)$ is referred to as the frequency response function (FRF) matrix.

The element $h_{ij}(s)$ of $H(s)$ can be written

$$h_{ij}(s) = \frac{b_1 s^{2n-2} + b_2 s^{2n-1} + \ldots + b_{2n-1} s + b_{2n-2}}{\det(B(s))} \tag{A-5}$$

For an n-dimensional system there will be $2n$ roots of the equation

$$\det(B(s)) = 0 \tag{A-6}$$

and if these roots are distinct, then $H(s)$ can always be written in the partial fraction form

$$H(s) = \sum_{k=1}^{2n} \frac{a_k}{(s-p_k)} \tag{A-7}$$

where

p_k = kth root of Equation (A-6)

a_k = residue matrix for the kth root

When the system is subcritically damped, as are practically all structures, the roots p_k occur in complex conjugate pairs, which can thus be written in the form

$$p_k = -\sigma_k + i\omega_k \quad , \quad p_k^* = -\sigma_k - i\omega_k \tag{A-8}$$

Modal vectors, u_k , are defined as solutions to the homogeneous equation

$$B(p_k)u_k = 0 \tag{A-9}$$

and, in terms of these modal vectors, the transfer matrix can be written in the form

$$H(s) = \sum_{k=1}^{2n} \frac{u_k u_k^T}{s-p_k} \tag{A-10}$$

or

$$H(s) = \sum_{k=1}^{n} \left[\frac{u_k u_k^T}{(s-p_k)} + \frac{u_k^* u_k^{*T}}{(s-p_k^*)} \right] \tag{A-11}$$

From Equation (A-10) or Equation (A-11) it may be seen that each row and each column of the transfer matrix (and, hence, the FRF matrix) contains each modal vector multiplied by a component of itself. Thus, if the effect of a single root could be isolated from the effect of all the other roots, the mode u_k should be identifiable from any row or column of the resulting $H_k(s)$, where

$$H_k(s) = \frac{u_k u_k^T}{s-p_k} \tag{A-12}$$

except those rows and columns corresponding to null elements of u_k . References 2 through 4 describe various methods for attempting to isolate the contribution, H_k , of a single mode in order to identify the elements of the modal vector u_k .

8. Selected References

1. A. L. Klosterman, "Modal Surveys of Weakly Coupled Systems," SAE Paper No. 760876, Nov. 1976.
2. A. L. Klosterman and R. Zimmerman, "Modal Survey Activity Via Frequency Response Functions," SAE Paper No. 751068, Nov. 1975.
3. M. Richardson, "Modal Analysis Using Digital Test Systems," Seminar on Understanding Digital Control and Analysis in Vibration Test Systems, Shock and Vibration Information Center, 1975.
4. R. J. Allemang, Investigation of Some Multiple Input/Output Frequency Response Function Experimental Modal Analysis Techniques, Ph.D. Thesis, U. of Cincinnati, 1980.
5. M. Richardson and J. Kniskern, "Identifying Modes of Large Structures from Multiple Input and Response Measurements," SAE Paper No. 760875, Nov. 1976.
6. G. W. Asher, "A Method of Normal Mode Excitation Utilizing Admittance Measurements," Proc. National Specialists' Meeting on Dynamics and Aeroelasticity, Inst. of Aeronaut. Sci., 1958, pp. 69-76.
7. R. R. Craig, Jr. and Y-W.T. Su, "On Multiple Shaker Resonance Testing," AIAA Journal, v. 12, n. 7, 1974, pp. 924-931.
8. R. R. Gold and W. L. Hallauer, Jr., "Modal Testing with Asher's Method Using a Fourier Analyzer and Curve Fitting,"

Proc. 25th International Instrumentation Symposium, Inst. Soc. Am., May, 1979, pp. 185-192.

9. C. Beatrix, Experimental Determination of the Vibratory Characteristics of Structures, ONERA Technical Note No. 212, 1973.

10. P. Ibáñez, "Force Appropriation by Extended Asher's Method," SAE Paper No. 760873, Nov. 1976.

11. R. R. Ensminger and M. J. Turner, "Structural Parameter Identification from Measured Vibration Data," AIAA/ASME/ASCE/AHS 20th SDM Conference, April 1979, pp. 410-416.

12. R. C. Lewis and D. L. Wrisley, "A System for the Excitation of Pure Natural Modes of Complex Structures," J. Aero. Sci., v. 17, n. 11, 1950, pp. 705-722.

13. R. R. Craig, Jr. and Y-T. Chung, Modal Analysis Using a Fourier Analyzer, Curve-Fitting, and Modal Tuning, Report No. CAR 81-1, Center for Aeronautical Research, Bureau of Engineering Research, The Univ. of Texas at Austin, Oct. 1981.

m'	f_1	ϕ_1	f_2	ϕ_2
1.000	1.0000	$\begin{Bmatrix} 1.000 \\ 1.000 \end{Bmatrix}$	1.0002	$\begin{Bmatrix} 1.0000 \\ -1.0000 \end{Bmatrix}$
1.001	0.9994	$\begin{Bmatrix} 1.0000 \\ 1.6176 \end{Bmatrix}$	1.0016	$\begin{Bmatrix} -1.6192 \\ 1.0000 \end{Bmatrix}$
1.010	0.9910	$\begin{Bmatrix} 1.0000 \\ 10.0098 \end{Bmatrix}$	1.0011	$\begin{Bmatrix} -10.1099 \\ 1.0000 \end{Bmatrix}$
1.100	0.9100	$\begin{Bmatrix} 1.0000 \\ 91.0100 \end{Bmatrix}$	1.0010	$\begin{Bmatrix} -100.1109 \\ 1.0000 \end{Bmatrix}$

Table 1. Effect of Subsystem Properties on System Modes of a Weakly Coupled 2DOF System.

Estimated Roots H_{11}

Root	Frequency	Damping	Amplitude	Phase
1	115.2	0.4707E-01	32.19	0.1799E-05
2	115.0	0.9298E-02	2.799	-0.1945E-05
3	119.0	0.2640E-02	104.4	1.684
4	119.5	0.5844E-02	11.33	0.2844
5	124.8	0.2241E-01	10.46	-3.142
6	124.8	0.5535E-02	0.2597E-02	0.7300E-04

Estimated Roots H_{21}

Root	Frequency	Damping	Amplitude	Phase
1	115.1	0.3076E-01	20.96	-0.2731E-05
2	115.0	0.6774E-02	1.287	0.2747E-05
3	119.0	0.2638E-02	105.5	1.692
4	119.4	0.6918E-02	12.86	0.7228E-01
5	124.8	0.1989E-01	8.361	3.142
6	124.8	0.4153E-02	0.4751E-02	-0.2091E-03

Estimated Roots H_{51}

Root	Frequency	Damping	Amplitude	Phase
1	115.0	0.8869E-02	0.9159E-01	0.1025E-05
2	119.0	0.2248E-02	21.34	1.479
3	119.6	0.2688E-02	21.75	-1.693
4	121.8	0.2591E-01	0.8192	-1.075
5	124.8	0.2374E-01	0.9778	-0.2076E-06

Estimated Roots H_{61}

Root	Frequency	Damping	Amplitude	Phase
1	115.0	0.1177E-01	0.1757	0.1314E-04
2	119.1	0.2258E-02	22.18	1.438
3	119.1	0.2723E-01	1.053	0.2236
4	119.6	0.2839E-02	22.71	-1.742
5	124.8	0.1433E-01	0.1876	-0.2673E-05

Table 2. MDOF Curve Fit Parameters for FRF's of Dual Beam Model

Estimated Roots H_{16}

Root	Frequency	Damping	Amplitude	Phase
1	115.2	0.4602E-01	2.207	-0.3383E-05
2	115.1	0.3774E-01	0.1315E-06	-2.032
3	115.0	0.3210E-02	0.4392E-02	0.2486E-03
4	118.9	0.2873E-02	12.55	1.589
5	120.0	0.2840E-02	13.00	-1.568
6	124.8	0.1538E-01	0.2645	-0.3002E-06

Estimated Roots H_{26}

Root	Frequency	Damping	Amplitude	Phase
1	115.3	0.6888E-01	1.838	0.4750E-06
2	115.0	0.3831E-02	0.3873E-01	-0.1847E-05
3	118.9	0.2962E-02	12.19	1.589
4	120.0	0.3257E-02	12.75	-1.572
5	124.8	0.1951E-01	0.5839E-07	-0.8005E-01
6	124.8	0.1038E-01	0.1001	-0.3857E-06

Estimated Roots H_{56}

Root	Frequency	Damping	Amplitude	Phase
1	115.0	0.1351E-01	5.757	0.1010E-05
2	118.8	0.3026E-02	105.2	1.591
3	119.7	0.9514E-02	0.3043E-02	-1.827
4	120.5	0.2598E-01	17.09	-0.9058
5	124.8	0.7826E-02	1.399	-3.142

Estimated Roots H_{66}

Root	Frequency	Damping	Amplitude	Phase
1	115.0	0.9683E-02	2.987	0.3488E-05
2	118.8	0.3012E-02	104.0	1.592
3	119.4	0.2926E-01	22.91	-0.7715
4	119.8	0.3661E-02	0.7704E-01	-2.299
5	124.8	0.9513E-02	2.130	3.142

Table 2.(Cont.) MDOF Curve Fit Parameters for FRF's of Dual Beam Model

BW (Hz)	SA f_1 (Hz)	SA Mode 1 Pt.	SA Mode 1 Ampl.	SA Mode 1 Phase	MCR f_1	MCR Mode 1 Pt.	MCR Mode 1 Ampl.	MCR Mode 1 Phase
10	118.789	1	1.000	0.0^{o}	118.789	1	1.000	-6.1^{o}
		2	0.931	-0.8^{o}		2	0.940	-5.8^{o}
		5	10.041	-1.9^{o}		5	8.697	-1.9^{o}
		6	9.926	-1.9^{o}		6	8.589	-1.9^{o}
4.0	118.804	1	1.0000	0.0^{o}	118.804	1	1.0000	-1.0^{o}
		2	0.934	-0.6^{o}		2	0.935	-0.5^{o}
		5	9.277	-0.4^{o}		5	9.063	-0.4^{o}
		6	9.167	-0.5^{o}		6	8.954	-0.5^{o}
1.0	118.802	1	1.000	0.0^{o}	118.802	1	1.000	-0.4^{o}
		2	0.934	-0.6^{o}		2	0.934	-0.1^{o}
		5	9.377	-0.1^{o}		5	9.283	-0.1^{o}
		6	9.267	-0.2^{o}		6	9.174	-0.2^{o}
0.256	118.801	1	1.000	0.0^{o}	118.801	1	1.000	-0.3^{o}
		2	0.933	-0.6^{o}		2	0.934	-0.3^{o}
		5	9.427	0.0^{o}		5	9.363	0.0^{o}
		6	9.316	0.0^{o}		6	9.253	0.0^{o}

Table 3. Effect of Analysis Bandwidth on Standard Asher and Minimum Coincident Response Modes.

BW (Hz)	SA				MCR			
	f_1 (Hz)	Mode 2			f_1	Mode 2		
		Pt.	Ampl.	Phase		Pt.	Ampl.	Phase
10	119.023	1	1.000	0.0^0	119.023	1	1.000	-1.0^0
		2	1.001	0.0^0		2	1.003	-0.9^0
		5	0.200	-34.6^0		5	0.048	-41.9^0
		6	0.193	-17.3^0		6	0.043	-40.0^0
4.0	119.024	1	1.000	0.0^0	119.024	1	1.000	-1.0^0
		2	1.001	0.0^0		2	1.003	-0.9^0
		5	0.197	-34.7^0		5	0.048	-42.0^0
		6	0.191	-17.1^0		6	0.043	-40.2^0
1.0	119.025	1	1.000	0.0^0	119.029	1	1.000	0.0^0
		2	1.002	0.0^0		2	1.003	0.0^0
		5	0.143	-36.2^0		5	0.036	-48.1^0
		6	0.138	-10.6^0		6	0.035	-48.5^0
0.256	119.027	1	1.000	0.0^0	119.029	1	1.000	-0.1^0
		2	1.002	0.0^0		2	1.003	0.0^0
		5	0.101	-38.2^0		5	0.037	-47.6^0
		6	0.098	-0.3^0		6	0.036	-47.9^0

Table 3(cont.). Effect of Analysis Bandwidth on Standard Asher and Minimum Coincident Response Modes.

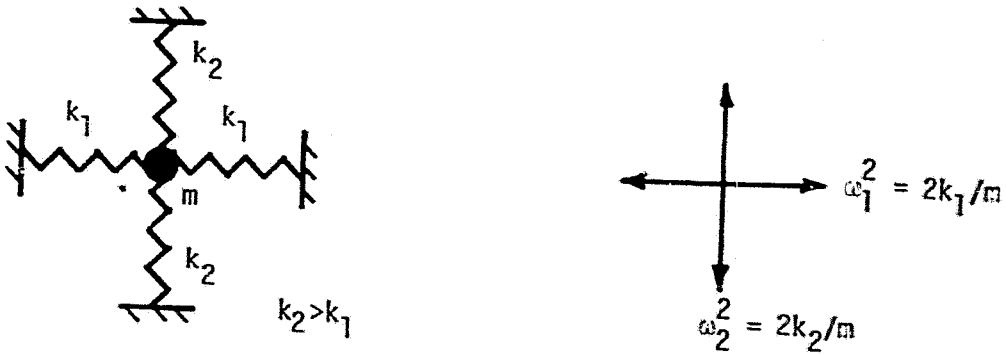

(a) 2DOF System with Unique Frequencies

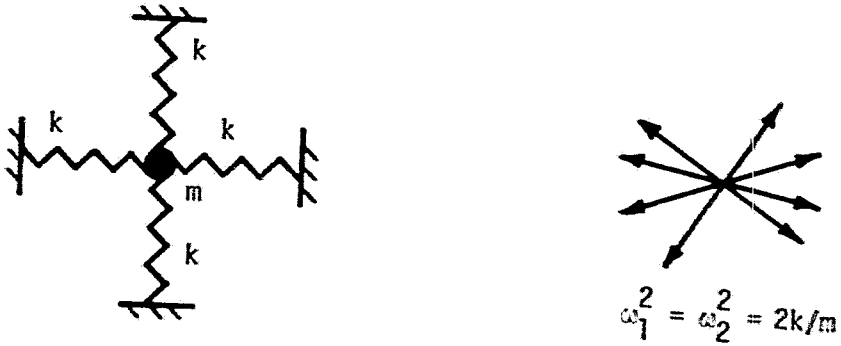

(b) 2DOF System with Repeated Frequencies

Figure 1. Systems with Unique Frequencies and with Repeated Frequencies.

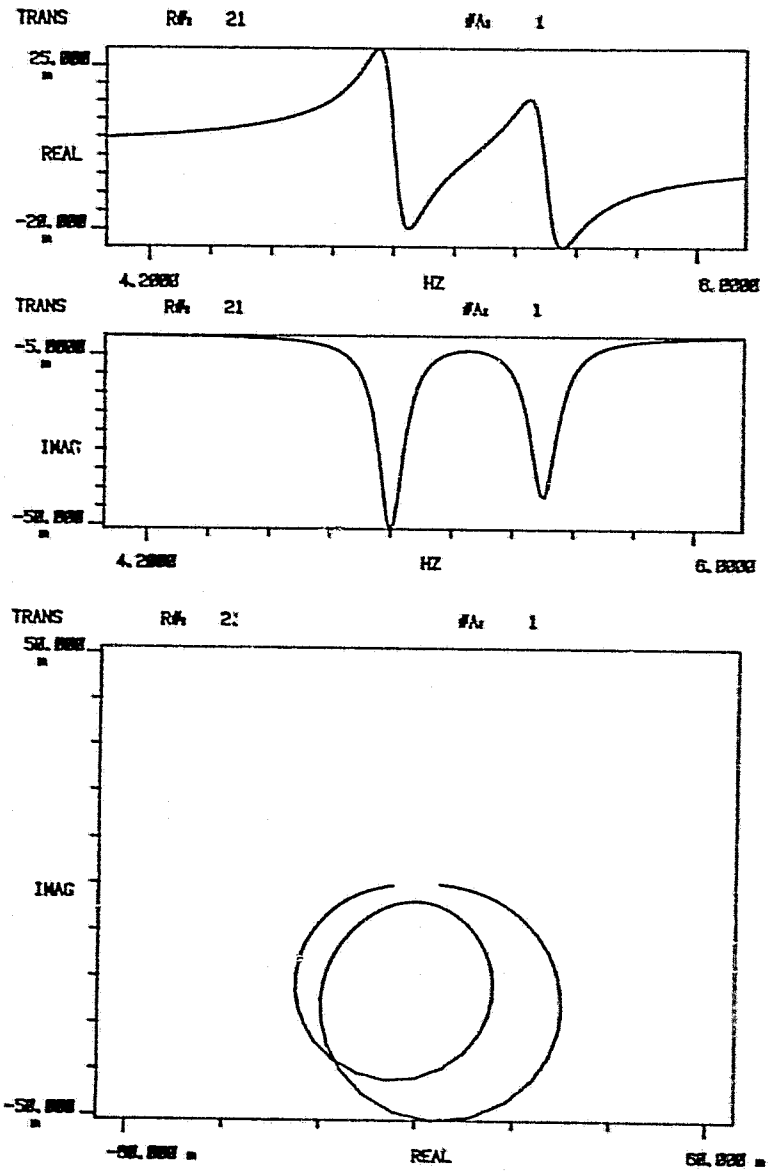

(a) 2DOF System with moderately spaced frequencies

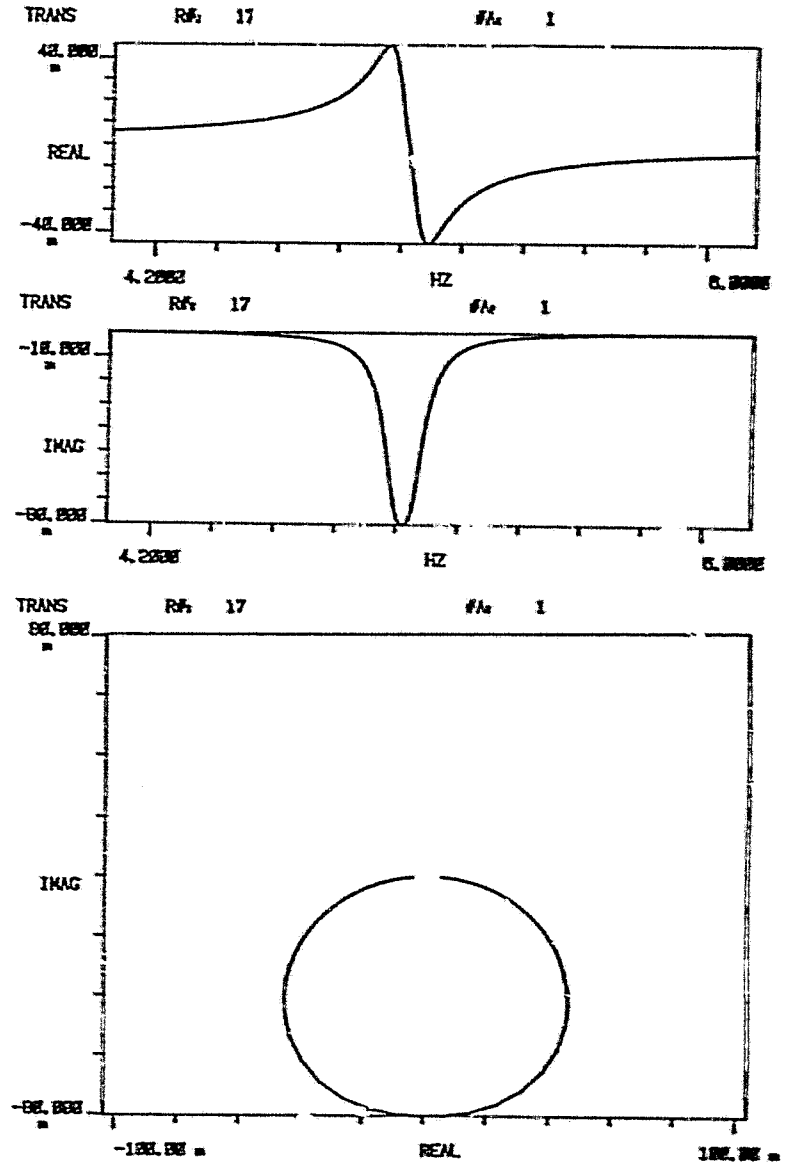

(b) 2DOF System with very closely spaced frequencies

Figure 2. Frequency Response Function H_{11} for 2DOF Systems.

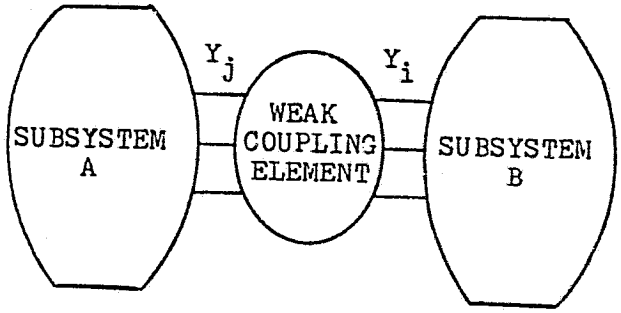

(a) Weakly coupled system with a weak coupling element

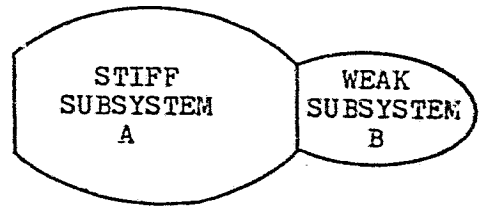

(c) Weakly coupled system with stiff and weak subsystem

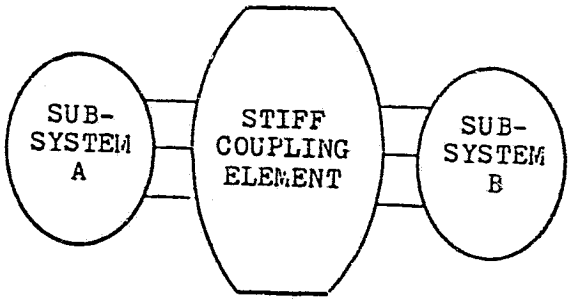

(b) Weakly coupled system with a stiff coupling element

Figure 3. Weakly-Coupled Systems Identified by Klosterman

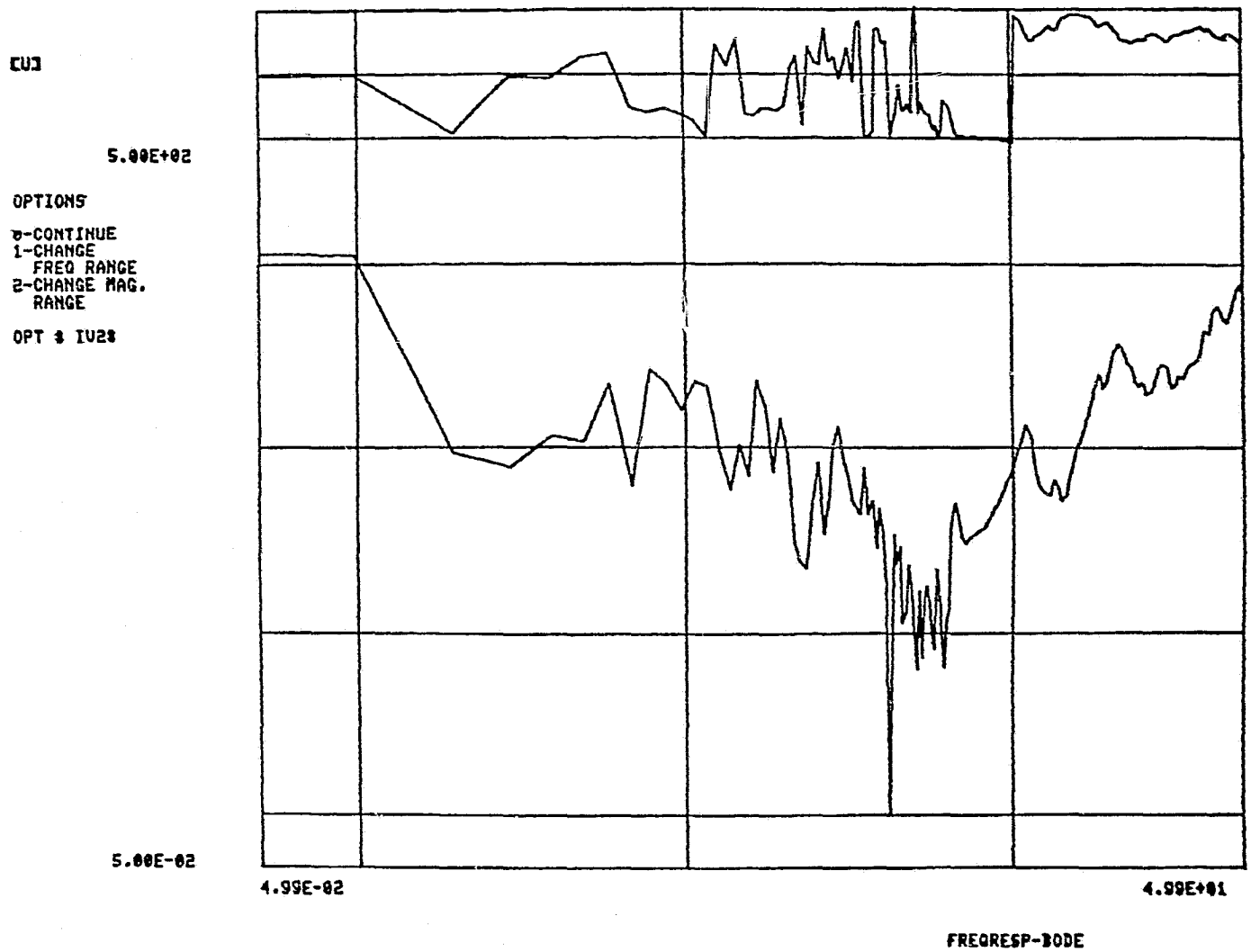

Figure 4. Bode Plot of Drive Point FRF of System with Closely-Spaced-Frequency Modes

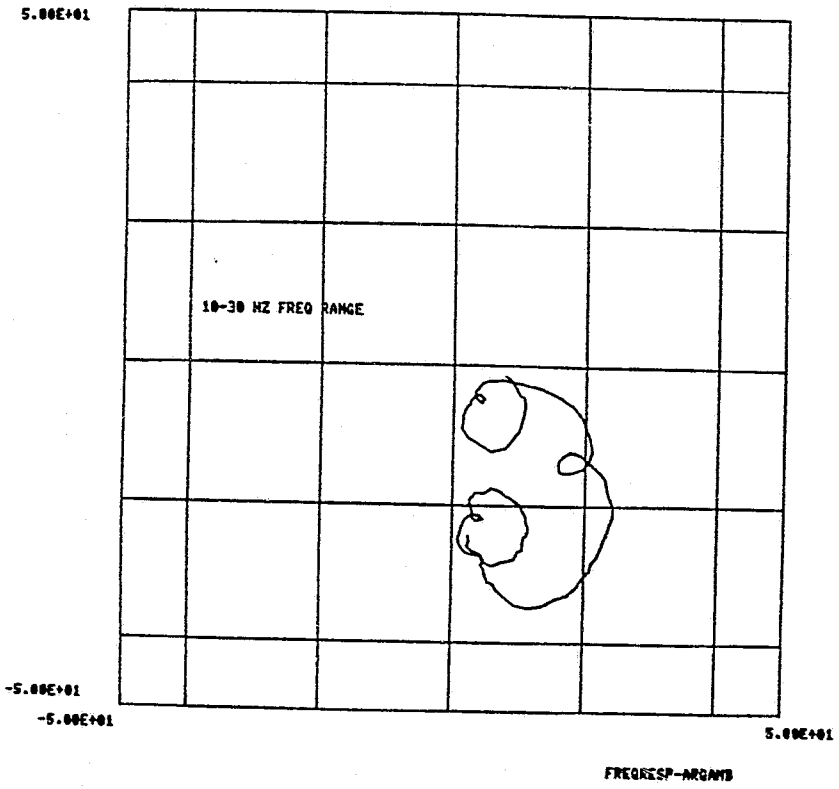

(a) Drive-point FRF

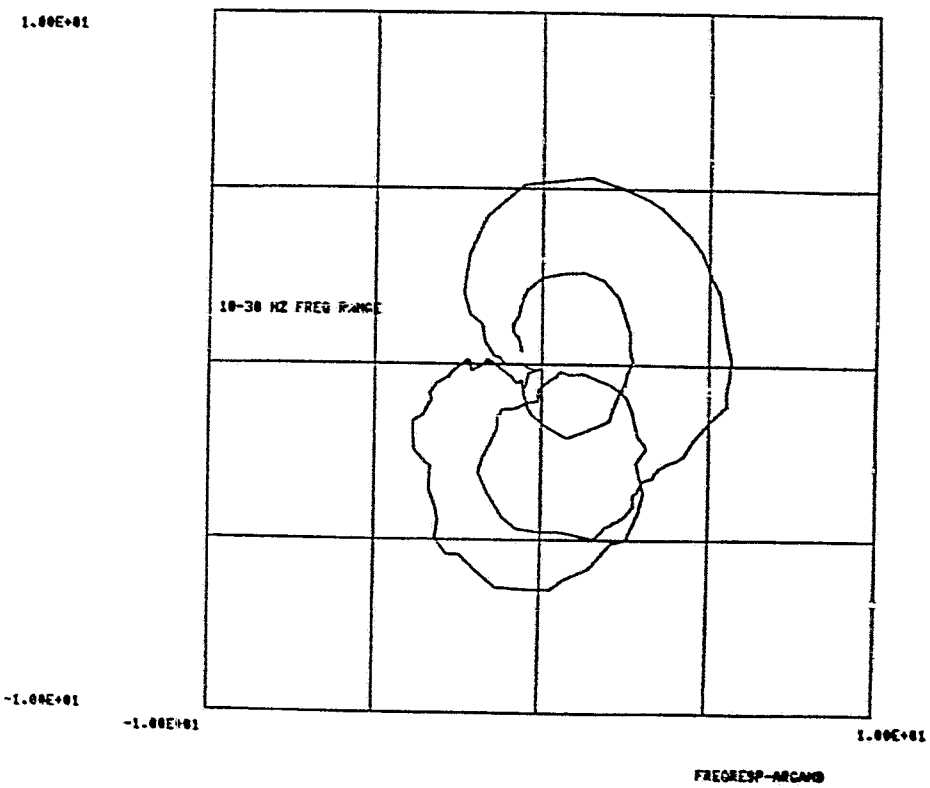

(b) Cross FRF

Figure 5. Argand Plots of Drive-point FRF and Cross FRF of System with Closely-Spaced-Frequency Modes

$$f_1 \;,\; \phi_1 = \begin{Bmatrix} 1.000 \\ 1.000 \end{Bmatrix}$$

$$f_2 \;,\; \phi_2 = \begin{Bmatrix} 1.000 \\ -1.000 \end{Bmatrix}$$

(a) Exact modes

$$f_1 = 4.998 \text{ Hz}, \quad \phi_1 = \begin{Bmatrix} 1.000 \\ 0.981 \end{Bmatrix}$$

$$f_2 = 5.502 \text{ Hz}, \quad \phi_2 = \begin{Bmatrix} 1.000 \\ -0.977 \end{Bmatrix}$$

(b) Quadrature response modes;*

f_1=5Hz, f_2=5.5Hz; shaker at 1.

$$f_1 = 4.985 \text{ Hz}, \quad \phi_1 = \begin{Bmatrix} 1.000 \\ 0.425 \end{Bmatrix}$$

$$f_2 = 5.059 \text{ Hz}, \quad \phi_2 = \begin{Bmatrix} 1.000 \\ -0.390 \end{Bmatrix}$$

(c) Quadrature response modes;*

f_1=5Hz, f_2=5.05Hz; shaker at 1.

$$f_1 = 4.985 \text{ Hz}, \quad \phi_1 = \begin{Bmatrix} 0.425 \\ 1.000 \end{Bmatrix}$$

$$f_2 = 5.059 \text{ Hz}, \quad \phi_2 = \begin{Bmatrix} -0.390 \\ 1.000 \end{Bmatrix}$$

(d) Quadrature response modes;*

f_1=5Hz, f_2=5.05Hz; shaker at 2.

Figure 6. "Modes" of 2DOF Systems

*Frequencies based on cross-FRF quadrature peaks.

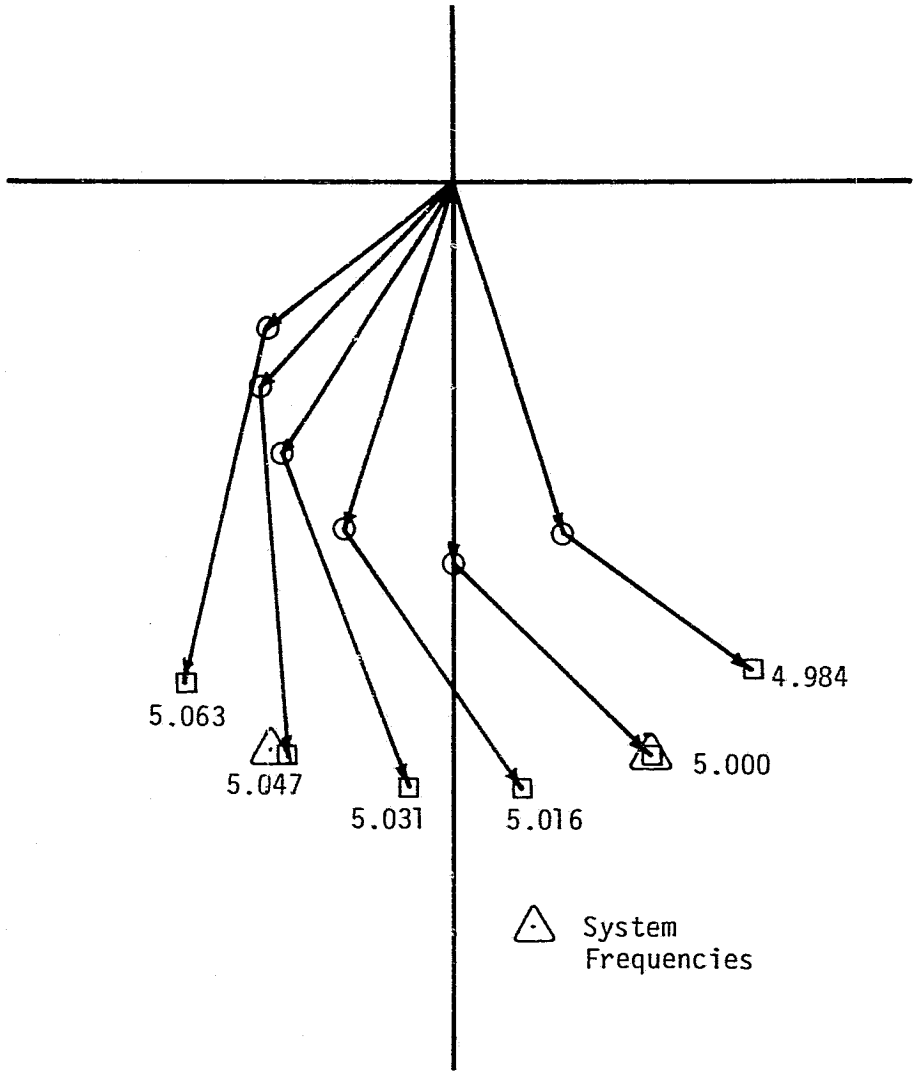

(a) H_{11} superposition components

Figure 7. Superposition of Frequency Responses of Closely-Spaced-Frequency Modes

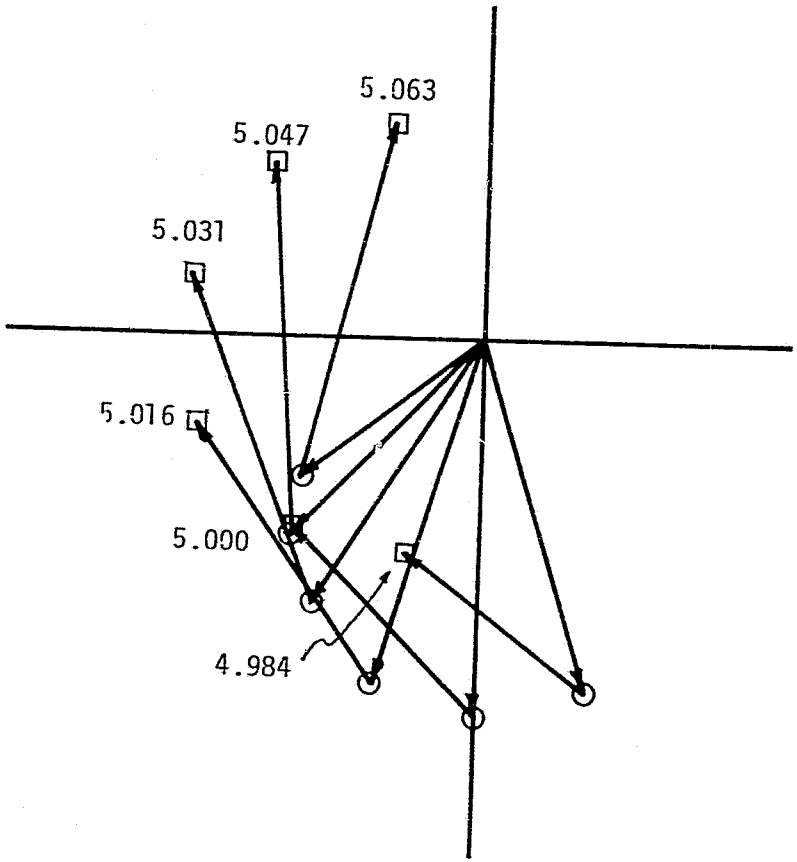

(b) H_{21} superposition components

Figure 7. Superposition of Frequency Responses of Closely-Spaced-Frequency Modes.

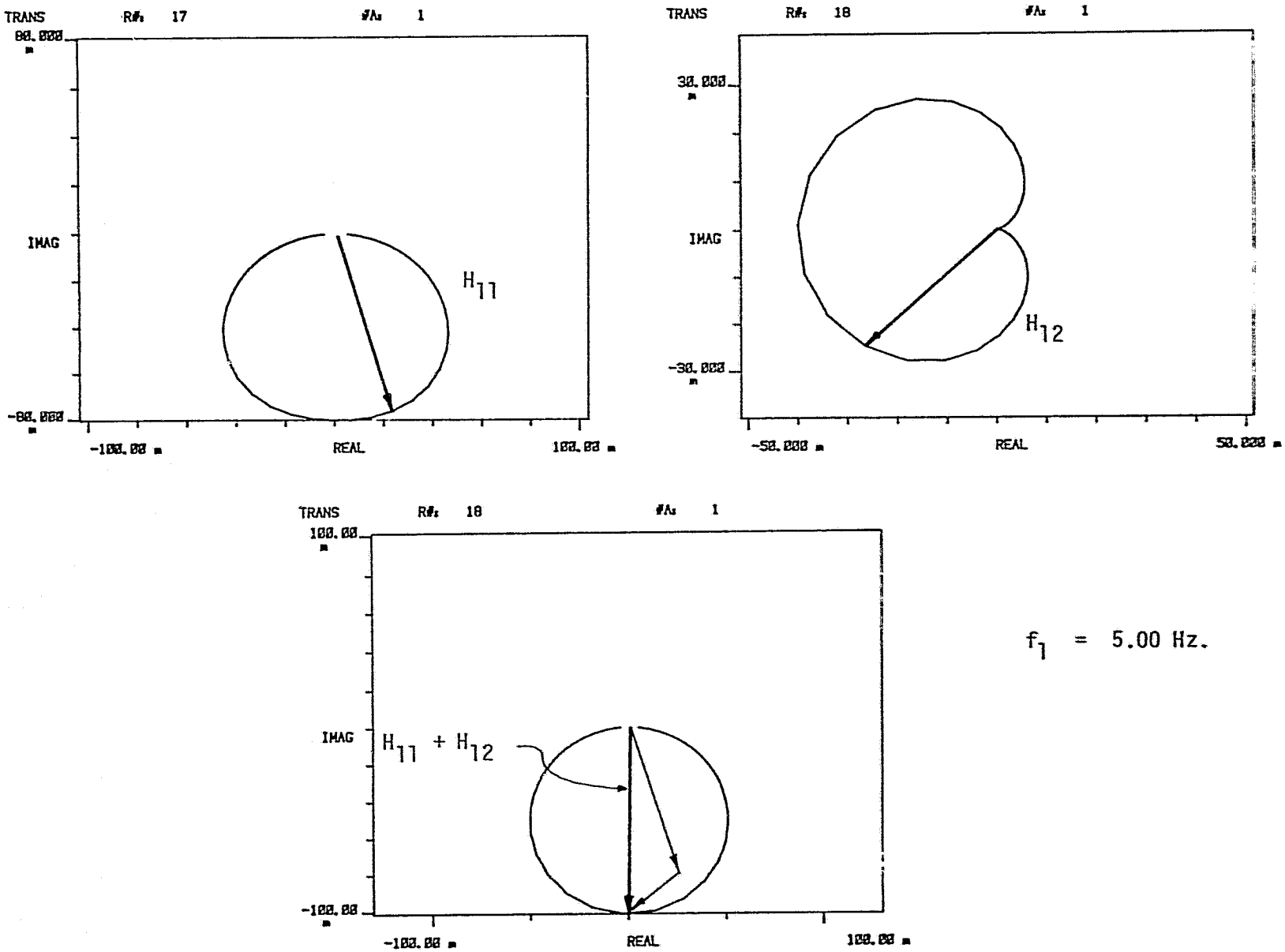

$f_1 = 5.00$ Hz.

Figure 8(a). Symmetry Averaging - $(H_{11} + H_{12})$

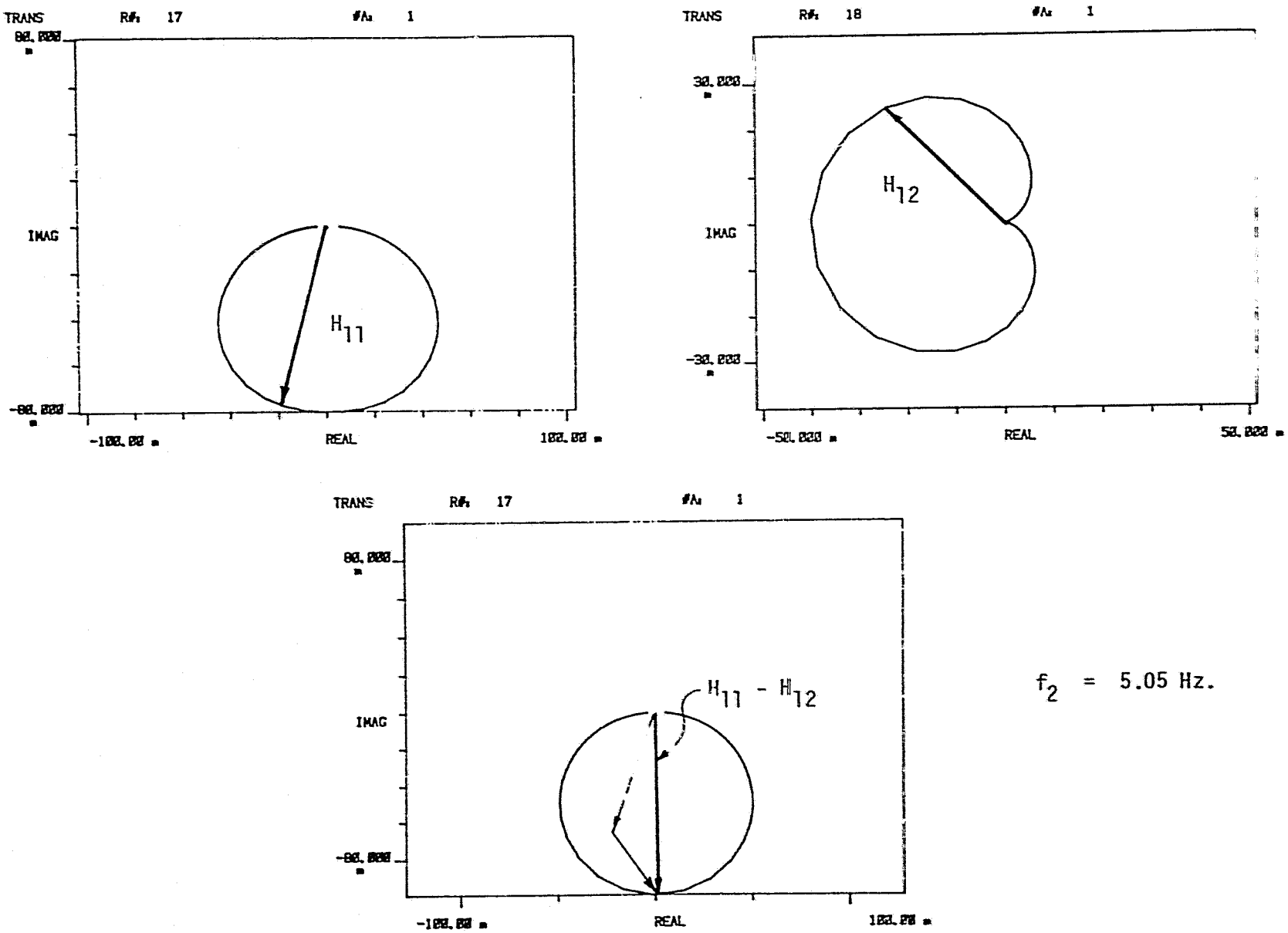

f_2 = 5.05 Hz.

Figure 8(b). Antisymmetry Averaging - $(H_{11} - H_{12})$

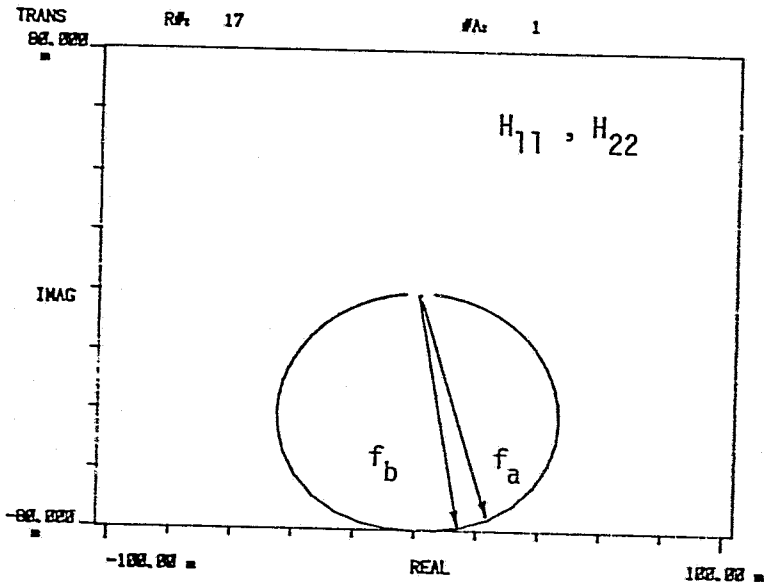

$$\det \begin{bmatrix} H_{11} & H_{12} \\ H_{21} & H_{22} \end{bmatrix}_R = 0$$

At f_a = 4.9934 Hz

$$\begin{vmatrix} 0.0316 & -0.0183 \\ -0.0187 & 0.0316 \end{vmatrix} = 0.00007$$

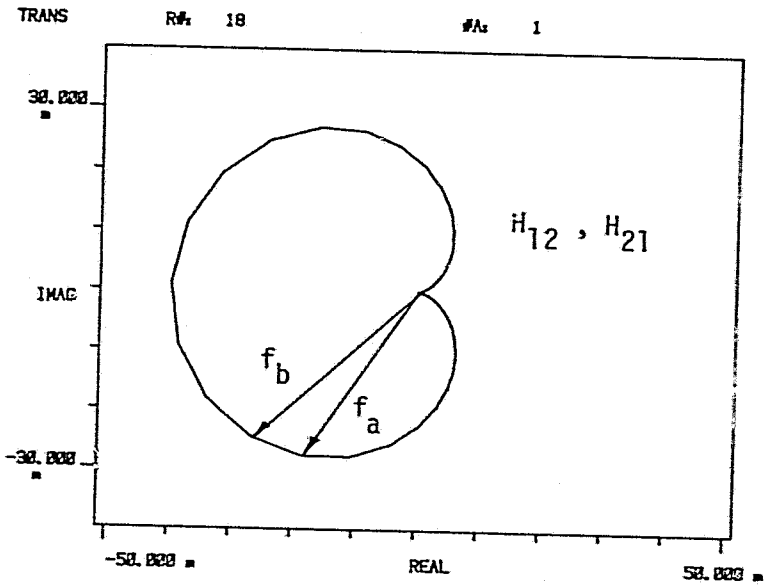

At f_b = 5.0016 Hz.

$$\begin{vmatrix} 0.0235 & -0.0266 \\ -0.0266 & 0.0235 \end{vmatrix} = -0.0002$$

Figure 9. "Mechanics" of Standard Asher Tuning - 5.0 Hz Mode

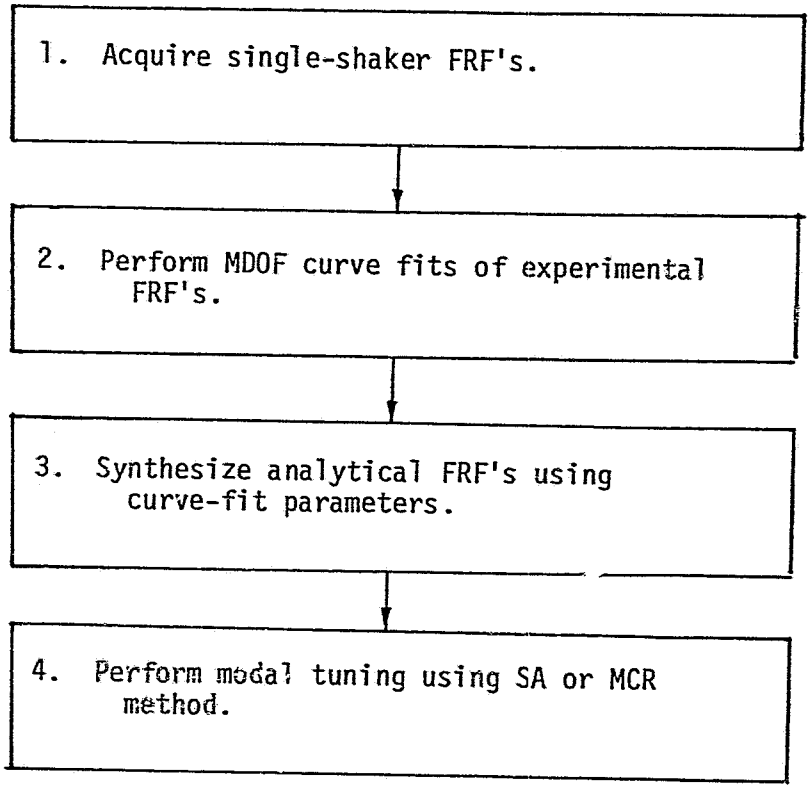

Figure 10. Modal Tuning Flow Chart

ORIGINAL PAGE
BLACK AND WHITE PHOTOGRAPH

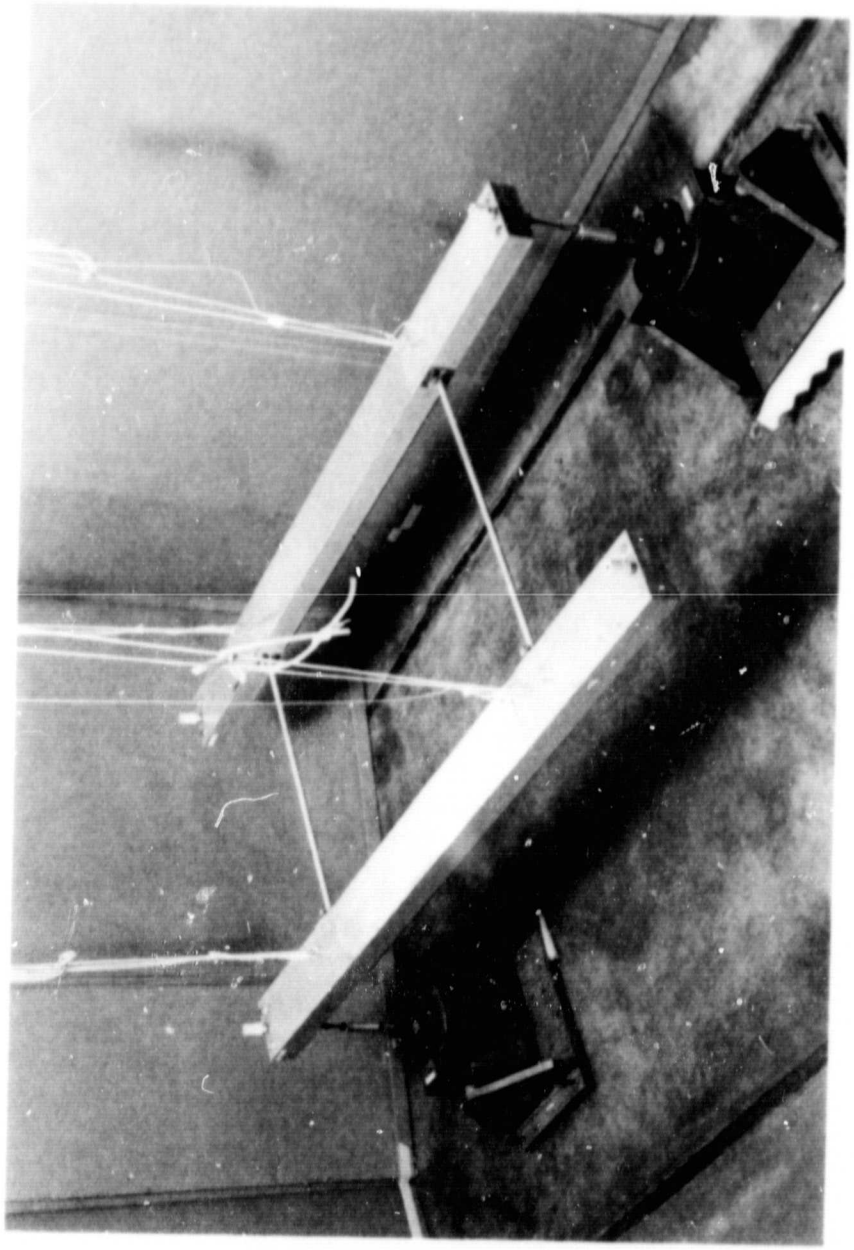

Figure 11. Weakly-Coupled Dual Beam System

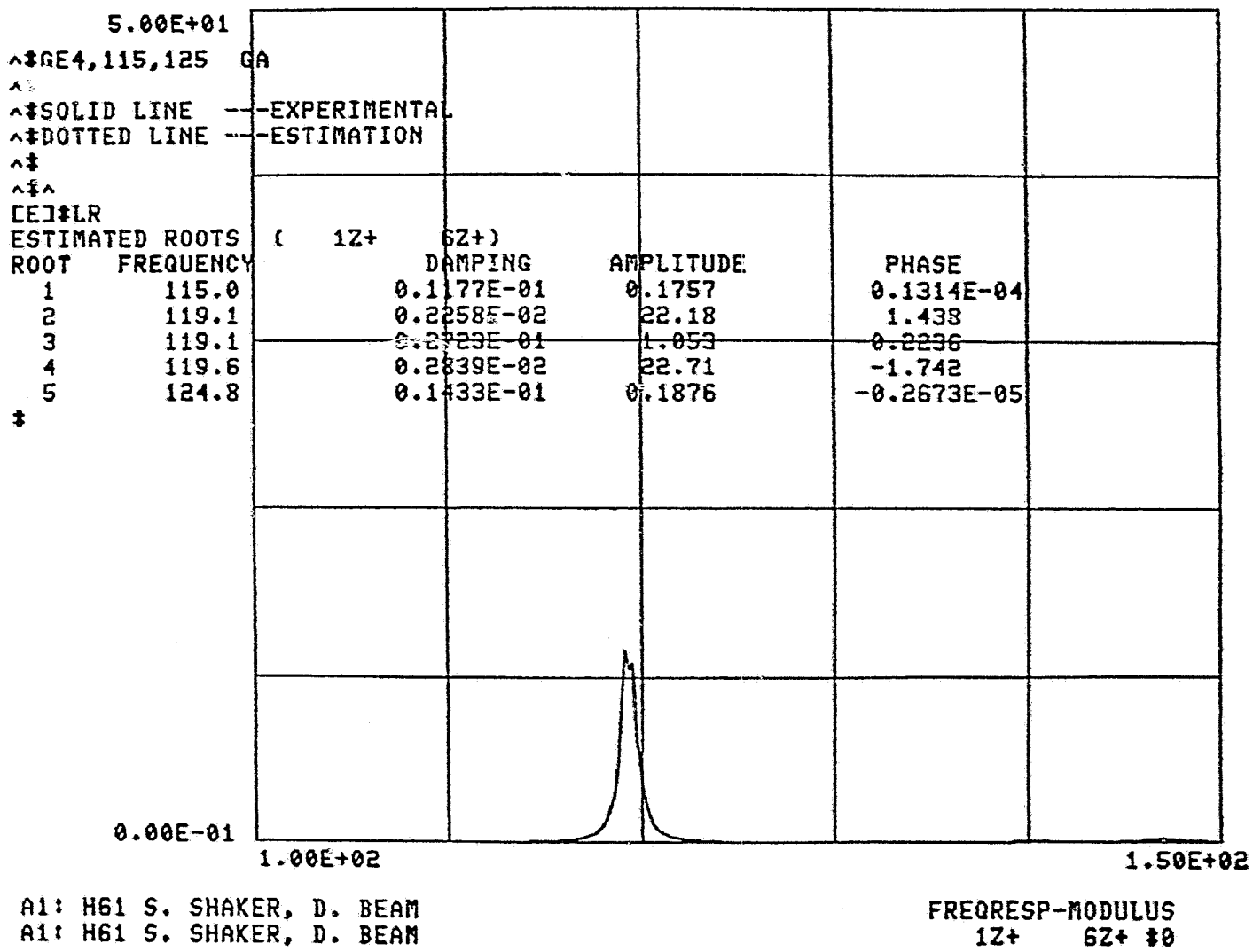

Figure 12. Typical MODAL-PLUS MDOF Curve Fit of Dual Beam FRF.

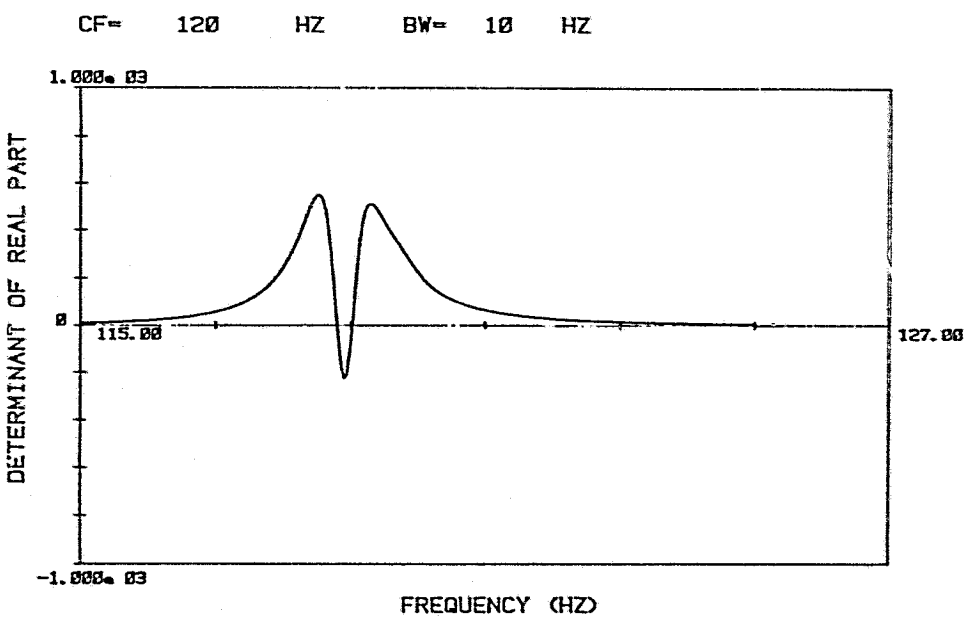

(a) SA Tuning

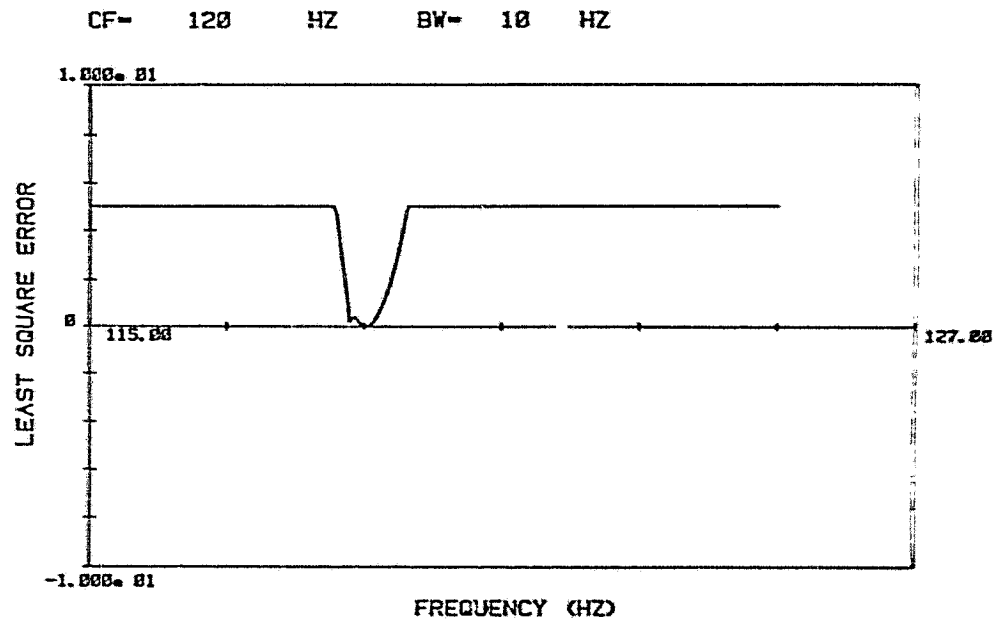

(b) MCR Tuning

Figure 13. Standard Asher and Minimum Coincident Response Modal Tuning Using 10 Hz Analysis Bandwidth

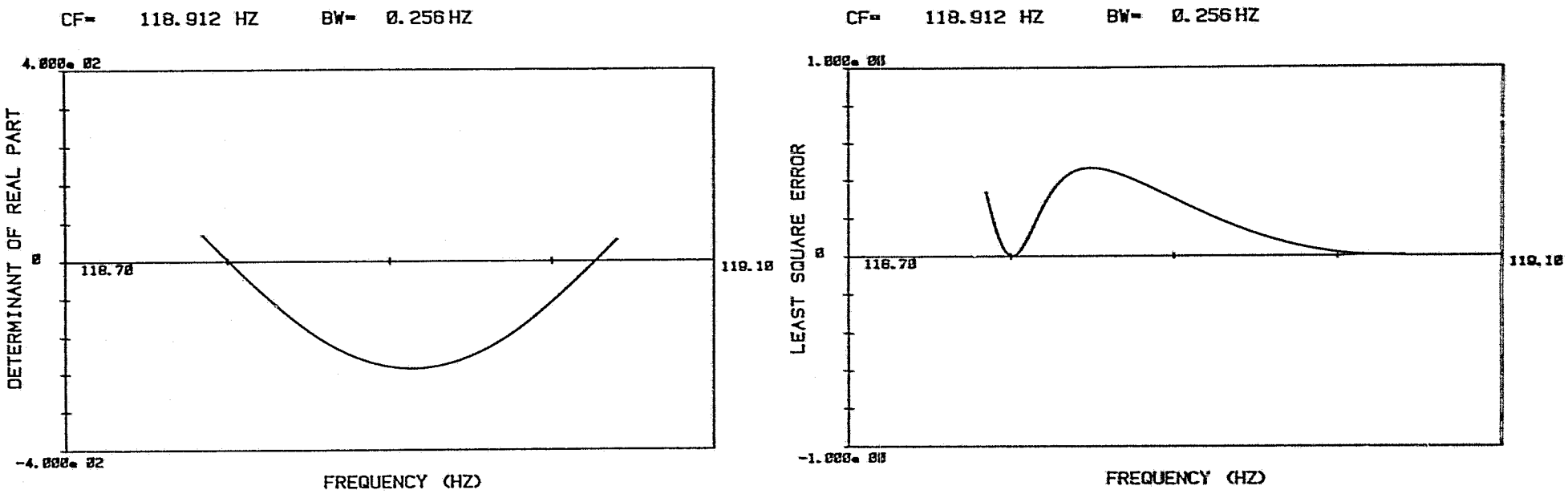

(a) SA Tuning

(b) MCR Tuning

Figure 14. Standard Asher and Minimum Coincident Response Modal Tuning Using 0.256 Hz Analysis Bandwidth